CrossMark

Effect of thermal history on nucleation and crystallization of poly(lactic acid)

Amirjalal Jalali[1], Michel A. Huneault[1,*], and Saïd Elkoun[2]

[1] *Department of Chemical and Biotechnological Engineering, Université de Sherbrooke, Sherbrooke, QC J1K 2R1, Canada*
[2] *Center for Innovations in Technological Ecodesign (CITÉ), Faculty of Engineering, Université de Sherbrooke, Sherbrooke, QC J1K 2R1, Canada*

ABSTRACT

In this paper, a successive heating and cooling protocol was designed to investigate the self-nucleation behavior of poly(lactic acid), PLA. The main objective of this investigation was to study the efficiency of the α and α' crystalline modifications of PLA. This was carried out by comparing crystallization temperatures upon cooling after self-nucleation of samples previously crystallized at various isothermal temperatures ranging from 80 to 130 °C. During heating to the partial melting range, three different mechanisms were observed for crystallized samples. For samples crystallized below 100 °C, an exothermic peak was detected prior the main melting peak which is ascribed to the α'–α solid-state transition. For samples crystallized between 100 and 120 °C, a melt recrystallization mechanism was observed. Finally, for samples crystallized above 120 °C, only melting of the α phase was detected. Upon cooling after partial melting, it was found that samples comprising a mixture of α and α' exhibited the highest crystallization temperature, the highest nuclei density, and the smallest spherulite size. Moreover, it was observed that samples that were isothermally crystallized between 100 and 120 °C, heated up to partial melting, and then cooled back to room temperature exhibited two peculiar crystallization peaks at 100 and 120° C. This phenomenon was ascribed to the formation of α and α' crystalline phases as revealed by X-ray diffraction. In addition, by slightly changing the temperature within the self-nucleation temperature range, a change of the proportion of each peak was observed.

Introduction

Poly(lactic acid) or PLA, is a biodegradable and biocompatible polymer that can be produced from renewable resources. It has raised particular attention as a potential replacement for petroleum-based polymers. Commercially available biobased PLA grades are generally made from a monomer mix containing mainly the *L*-enantiomer with small concentrations of *D-LA* impurities that can act as crystal defects. PLA

Address correspondence to E-mail: Michel.Huneault@USherbrooke.ca

exhibits high tensile modulus and strength, along with high transparency. Accordingly, this biobased polymer is a promising material for various applications such as textiles, bottles, thermoformed containers, paper, and cardboard coating. Due to its low glass transition temperature ($T_g \sim$ 60–65 °C), PLA has a low heat resistance unless it can be fully crystallized, and therefore, PLA crystallization has been a subject of great interest in the past decade [1]. Crystallization of this polymer is strongly dependent on D-content and is hindered as D-concentration increases. Furthermore, it suffers from low crystallization kinetics unless it is subjected to high orientations. Hence, increasing the crystallization rate in processing techniques, such as injection molding where orientation levels are relatively low, is required to improve its thermal resistance [2–9].

It is well understood that PLA is a polymorphous polymer. During the last decade, the crystal structure of PLA has attracted particular attention of researchers. It has been shown that PLA exhibits two different crystalline phases termed α and α'. By means of FTIR and WAXD analysis, α' was described as a disordered form of the stable α phase [10–15]. Differences between the crystalline structures were associated to chain conformation and chain packing mode between the disordered and ordered forms. It was found that crystallization at temperatures below 100 °C lead predominately to the α' crystalline form whereas at temperatures above 120 °C, the α phase was the main form [15, 16]. Within the 100–120 °C crystallization temperature range, a mixture of these crystalline phases was present. Different thermal properties for α' and α phases stem from the structural difference and interchain interactions. Equilibrium melting enthalpy, ΔH_m°, of α' crystals is 57 J/g which is 40 J/g lower than that of α, 96 J/g [17, 18].

The crystallization of PLA can be enhanced by the addition of nucleating agents and plasticizers or combination of both to increase nucleation density and chain mobility [1, 19]. From a crystallographic and chemical point of view, the self-seeded nuclei can be regarded as ideal nucleating agents for improving the crystallization of semi-crystalline polymers. Based on this assumption, Fillon et al. [20–24] developed a nucleation efficiency scale to measure the efficiency of heterogeneous nucleating agents for polypropylene. In this technique, the crystallization temperature of the investigated polymer formulation was compared to those obtained with the pure polymer and to the pure polymer subjected to a procedure known as self-nucleation. Self-nucleation was produced by first heating to the partial melting region, where the temperature is in the vicinity of the melting peak temperature. Then, by cooling down with a controlled cooling rate, the exothermal crystallization peak can be recorded. The highest crystallization temperature T_C^{max} found is taken as the upper limit for the nucleation efficiency scale.

Self-nucleation can also be employed as a convenient procedure to establish a relationship between crystallization and the microstructure of polymers. Nucleation behavior of poly(vinylidene fluoride), PVDF, in its α phase has been studied by Schneider et al. [25]. It was observed that the sample containing the highest number of defects after the self-nucleation exhibited the lowest crystallization temperature on subsequent cooling.

The successive and self-nucleation and annealing, (SSA), thermal fractionation has also been introduced by Müller et al. [26–28]. This technique involved successive self-nucleation and annealing steps and was used to characterize copolymers. SSA gives information on the distribution of short chain branching and lamellar thickness. In random copolymers, the second component disturbs the crystallization of the major element, and materials are sensitive to thermal fractionation.

A nucleation efficiency scale for PLA has been developed in the solution state by Schmidt and Hillmyer [29]. Upon cooling at 2 °C/min, T_C^{min} and T_C^{max} were 106 and 157 °C, respectively. In another study, Anderson and Hillmyer used the same procedure for the melt processed PLA [30]. By using a cooling rate of 5 °C/min, T_C^{min} and T_C^{max} were 104.3 and 142.9 °C, respectively. However, by changing the cooling rate to 2 °C/min, T_C^{max} shifted to 149 °C.

Isothermal and non-isothermal crystallizations of PLA were examined from the molten and glassy state by De Santis et al. [31]. Nucleation and growth rate of the formed crystals were calculated. Crystallization kinetics from the glassy state exhibited a faster rate than from the molten state. The kinetics of crystal formation of PLA at non-isothermal condition was examined at different cooling rates [32]. Although the crystallization of PLA took place on cooling the melt at rates lower than 0.5 Ks^{-1}, crystal nuclei shaped even at cooling rates up to 50 Ks^{-1}. Additionally,

decreasing the cooling rate led to increase the nuclei density.

In this contribution, a thermal protocol was designed to characterize and understand the self-nucleation mechanism of PLA. The work first aimed at better understanding the crystallization temperature on the formation of α and α′ crystals. Secondly, the α′ to α transition upon heating to self-nucleation range was investigated. Finally, the effect of these induced crystalline phases on self-nucleation was assessed. For this purpose, calorimetric, X-ray diffraction as well as optical microscopy was employed to investigate the crystallization behavior of PLA.

Experimental

Materials

A commercial PLA, grade 4032D supplied by NatureWorks, was used. This PLA is a semi-crystalline grade that contains 2 % D-LA. The measured weight-averaged molecular weight (M_w) and polydispersity index (M_w/M_n) of PLA were 109 kg/mol and 1.57, respectively [33].

Sample preparation

The main reason of this study was to find out the optimum crystallization kinetics for the crystallization of PLA in realistic condition in which PLA is processed in molten state. For this reason, the samples were extruded. Samples were prepared using a HAAKE Minilab conical twin screw micro compounder (Thermo Scientific). PLA was vacuum dried at 50 °C for 2 days prior to melt mixing. Mixing was carried out at 180 °C for 5 min at a rotation speed of 100 rpm. The extruded samples were also dried in the same conditions and prepared in a twin screw extruder at 180 °C at a mass flow rate of 20 kg/h.

Characterization

Thermal behavior: differential scanning calorimetry (DSC)

The thermal behavior of PLA samples was studied using a DSC Q2000 from TA Instruments. Temperature was calibrated before measurements using Indium as a standard material. Samples weight was kept constant in the range of 10–15 mg. The typical variation on crystallization and melting temperatures were assessed at ±0.2 °C, while the accuracy of crystallization and melting enthalpies were estimated at ±1.5 J/g.

Microstructural analysis: wide-angle X-ray diffraction analysis (WAXD)

Wide-angle X-ray diffraction (WAXD) patterns were obtained by means of an X-ray diffractometer (D-8, Bruker) to detect the crystalline phases at different crystallization temperatures. The samples were exposed to an X-ray beam with the X-ray generators running at 40 kV and 40 mA. The copper K_α radiation ($\lambda = 1.542$ Å) was selected, and the scanning was carried out at 0.03°/s in the angular region (2θ) of 5–40°.

Isothermal crystallization: hot-stage and optical microscopy

Isothermal crystallization experiments were performed by means of optical microscopy, Leica MDRX polarized, to observe the effect of isothermal crystallization on PLA crystalline morphology, and to measure nuclei density and growth rate. The samples were melted between two glass slides at 200 °C, and then the glasses were gently pressed to squeeze the melt into a very thin film. The prepared slides were moved onto a Mettler Toledo FP82HT hot-stage (UNITRON Bi-9691), kept at 200 °C for 3 min, then quenched to 130 °C, and finally held at that temperature to monitor the spherulite growth rate in isothermal condition.

Results and discussion

PLA self-nucleation: cooling rate and thermal protocol effect

For most semi-crystalline polymers, the heating and cooling rates in calorimetric experiments is around 10 °C/min. Due to slow crystallization kinetics of PLA, a cooling rate of 10 °C/min is too high to detect any crystallization peak. Hence, selecting the appropriate scanning rate for PLA is a crucial parameter in a study on the self-nucleation behavior of PLA. Figure 1 presents the cooling curves after maintaining PLA
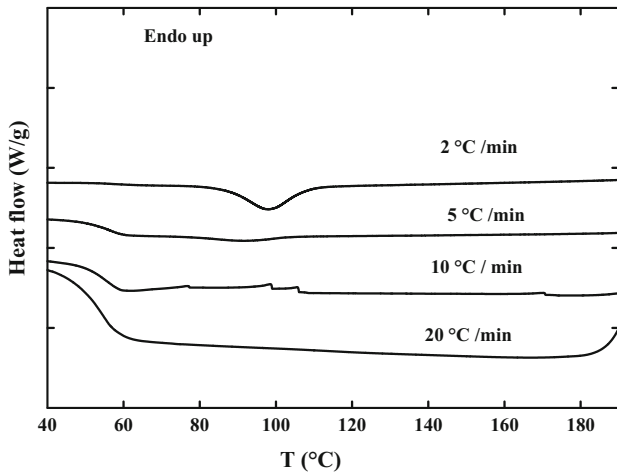
Figure 1 DSC curves for PLA at different cooling rates after holding at 200 °C for 5 min.

Figure 2 Schematic representation of temperature protocol for the self-nucleation of PLA. *A* Erasing thermal history, *B* Isothermal crystallization, *C* Partial melting, *D* Cooling down, *E* Final heating, T_{iC} Isothermal crystallization temperature, T_S Self-nucleation temperature.

Figure 3 DSC cooling scans at 2 °C/min for sample previously crystallized at $T_{iC} = 80$ °C then self-nucleated for 5 min at the indicated self-nucleation temperature, T_s (Segment D in Fig. 2).

sample at 200 °C for 5 min and subsequently cooling down at 20, 10, 5, and 2 °C/min, respectively. Upon cooling at 20 and 10 °C/min, no peak can be observed. At the cooling rate of 5 °C/min, a broad and weak crystallization peak was detected around 91 °C but the crystallization enthalpy is only 2.3 J/g. However, by decreasing the cooling rate to 2 °C/min, a clear and well-defined crystallization peak at approximately 98 °C was observed with a crystallization enthalpy of 25 J/g. Based on these results, a cooling rate of 2 °C/min was selected for the study of self-nucleation of PLA and, accordingly, to detect crystallization upon cooling within a reasonable time frame.

Figure 2 presents the protocol used to investigate the self-seeding of PLA. The sample was first heated up to 200 °C and held for 5 min to erase thermal history. This is referred to as Segment A in Fig. 2. The sample was then quenched to a determined annealing temperature, T_{iC}, and held for a period, ranging from 1 to 4 h, until completion of crystallization. This is referred to as Segment B in Fig. 2. Afterward, the sample was heated up to the self-seeding range under the heating rate of 2 °C/min. Once at the self-nucleation or self-seeding, the temperature was held constant for 5 min. This is referred to as Segment C in Fig. 2 and has been used to assess the partial melting endotherm. To measure the crystallization temperature of the self-nucleated sample, the sample was cooled down to room temperature at 2 °C/min to detect the crystallization exotherm, which is referred to as Segment D in Fig. 2. Finally, to assess the
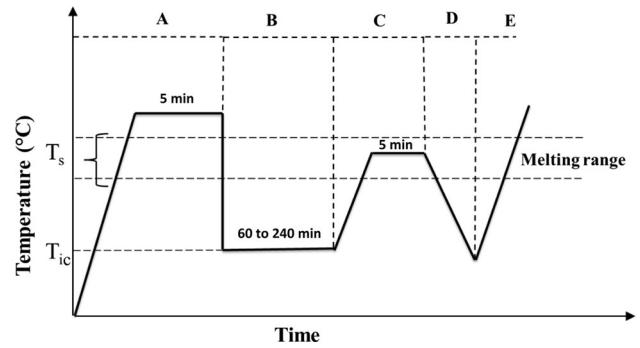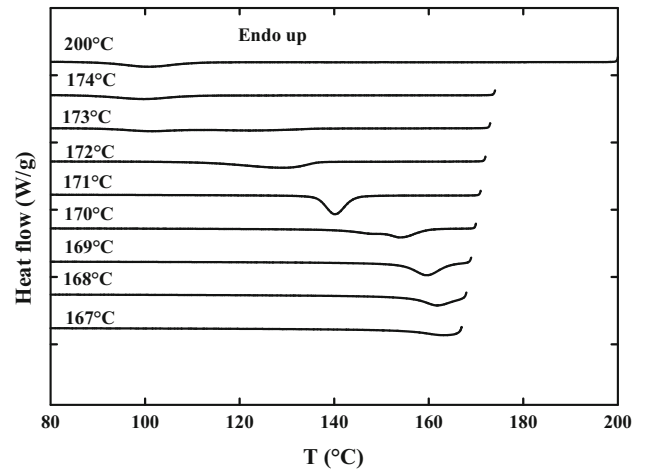
melting behavior and type of the crystal modification, the sample was reheated again in Segment E at 2 °C/min up to complete melting.

Isothermal crystallization at 80 °C

At first, self-nucleation of samples crystallized at 80 °C was examined. In these conditions, it took 4 h to complete the crystallization, and only the formation of α′ phase was expected. Figure 3 displays the DSC thermographs under cooling at 2 °C/min after self-nucleation at different temperatures, T_s. This corresponds to segment D in the thermal protocol presented previously (Fig. 2). Table 1 summarizes the transition temperatures and enthalpies obtained

Table 1 Crystallization temperature, enthalpies of crystallization and melting as a function of self-nucleation temperatures

T_s (°C)	T_{C1} (°C)	T_{C2} (°C)	ΔH_C (J/g)	T_{m1} (°C)	T_{m2} (°C)	ΔH_m (J/g)
167	163.5	–	–*	–	169	42
168	161.8	–	–*	167	170.3	44
169	159.4	–	37.3	168	170.5	45.2
170	153.9	148	48.7	–	169	47.8
171	140	–	42.7	–	170.6	53.5
172	129.2	–	39.7	173	175	52.6
173	122	101	34.2	173.3	175.2	59.5
174	99.9	–	24.2	–	175	58.4

* Not measurable

for T_s between 167 and 174 °C. For the samples molten at T_s equal to 174° C or higher, the obtained crystallization temperature after cooling remained constant at approximately 100 °C. The above 174 °C is called Domain **I**. In this region, nearly all crystal fragments were molten down, and since there was no self-nucleation, crystallization temperature was independent of T_s. In the 170 °C ≤ TS ≤ 174 °C region, the self-nucleation occurred, and the crystallization temperature increased as T_s decreased. This domain, known as Domain **II**, is characterized by the presence of very small crystal fragments whose concentrations vary with T_s. The presence of these very small crystals largely favors self-nucleation over annealing. This noticeable increase in crystallization temperature with the decreasing T_s can be ascribed to a significant increase in nucleation density associated with the higher concentration of residual crystal fragments. In addition, the enthalpy of crystallization, ΔH_C, increased as T_s decreased from 174 to 170 °C. A similar increase in ΔH_C upon decreasing T_s was reported for PET and poly(p-dioxanone), (PPDX), within Domain II [20, 34, 35]. The range of self-nucleation temperatures below 170 °C is called Domain **III**. In this region, although self-nucleation takes place, the annealing effect of existing crystals is the predominant mechanism.

Figure 4 depicts the larger scale of DSC cooling curves for T_s in Domain II. After self-nucleation at 170 °C, two crystallization peaks can be observed upon cooling. The first one is at 153.9 °C and the next small one is around 148.1 °C. Moreover, when temperature increased within this domain, a double exothermic crystallization peak was detected again after cooling from T_s = 173 °C. The first crystallization peak was observed at around 120 °C, and the second one was around 100 °C. The double
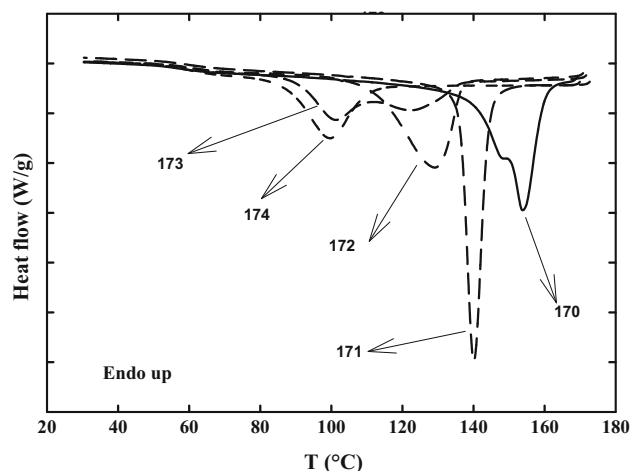

Figure 4 DSC enlarged cooling scans at 2 °C/min for sample previously crystallized at T_{iC} = 80 °C and then self-nucleated for 5 min at the indicated self-nucleation temperature, T_s (Segment D in Fig. 2).

crystallization peak can be ascribed to crystalline phases of PLA. This will be discussed in next sections.

In order to determine the frontiers of each domain, a subsequent heating scan after self-nucleation is required. Hence, a final heating at the rate of 2 °C/min was also carried out to further probe the structure developed upon cooling after self-seeding. This corresponds to segment E of the thermal protocol (Fig. 2). Figure 5 illustrates these heating scans. For most samples in Domain II, there were two melting peaks. The lower melting peak, changed with T_s, whereas the higher one was independent of T_s. The lower melting peak could be associated to the melting of crystals formed upon cooling from T_s, while the second endothermic peak could be ascribed to melt recrystallization of crystals taking place upon the heating process. For T_s in Domain III (i.e.,
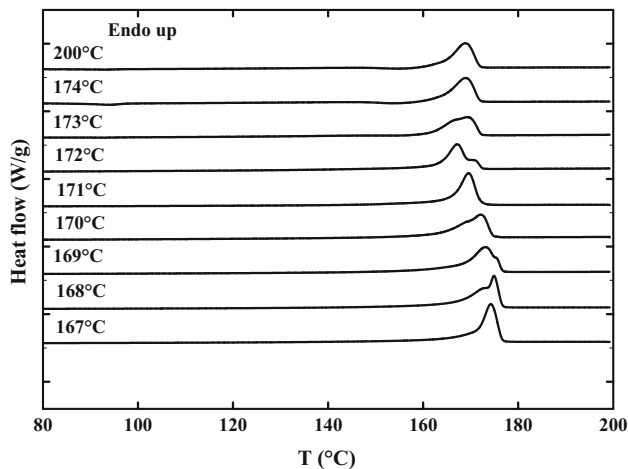
Figure 5 DSC heating scans at 2 °C/min after the cooling shown in Fig. 3. T_s values are indicated above each curve. (Segment E in Fig. 2).

Figure 6 XRD patterns of PLA at indicated isothermal crystallization temperatures.

$T_s < 170$ °C), two melting peaks were also observed. However, in this domain, crystal fragments are larger and annealing competes with self-nucleation and is more likely to happen as T_s decreases. Accordingly, the higher melting peak is ascribed to the annealing process during heating and the lower endothermic peak corresponds to melting of crystals that formed during cooling and recrystallizing upon heating.

Effect of crystalline phase on self-nucleation

Crystalline structure

Figure 6 presents the XRD patterns of PLA isothermally crystallized at 80, 115, and 130 °C, respectively. The XRD patterns of PLA crystallized at these temperatures were rather similar. For sample crystallized at 80 °C, where only the α′ phase was expected, two strong diffraction peaks were observed at 16.6° and 18.9°, corresponding to (110)/(200) and (203) planes [36]. These peaks shifted slightly to higher 2θ with crystallization temperature, T_{iC}, due to a decrease in lattice spacing. Additionally, for samples crystallized at 115 °C, where a mixture of α and α′ phases is expected, and at 130 °C, where only the α phase should be present, three small diffraction peaks at 12.5°, 15°, and 22° associated to the α phase appeared. Thus, these XRD patterns confirmed the gradual shift from the α′ to the α form with increasing isothermal crystallization temperature.
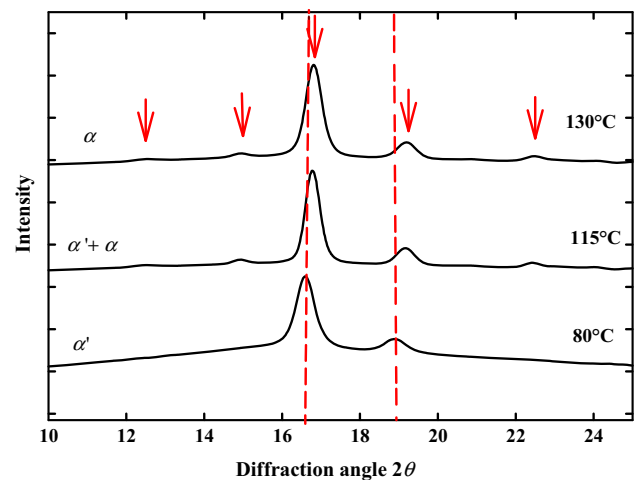
Self-nucleation of (α′ + α) and α phases

In order to investigate the effect of the crystalline phases developed upon the isothermal crystallization step on the subsequent self-nucleation experiments were repeated following isothermal crystallization at different temperatures, T_{ic}. As explained in the experimental section, the samples were quenched from the melt state to the desired isothermal crystallization temperature, held for sufficient time to complete the crystallization and subsequently reheated to the self-seeding range.

The DSC heating scans from the isothermal crystallization temperature to the self-seeding temperature were carried out and are shown in Fig. 7. This corresponds to segment C in Fig. 2. For $T_{iC} = 80$ and 100 °C, a small exotherm appeared prior to the main melting peak. However, for temperature inclusively between 105 and 120 °C, this exotherm was replaced by an endothermic peak. For PLA crystallized at 130 °C, no peak can be seen before the main melting peak. Three different mechanisms may be invoked. Indeed for samples crystallized at 100 °C or below, the observed exothermic peak is associated to a solid-state transition where disordered α′ phase transforms into the ordered α-phase [15]. For samples crystallized between 100 and 120 °C, α′-α transformation takes place through a melt recrystallization mechanism. Finally, for sample crystallized above 120 °C, no phase transition occurs [16].
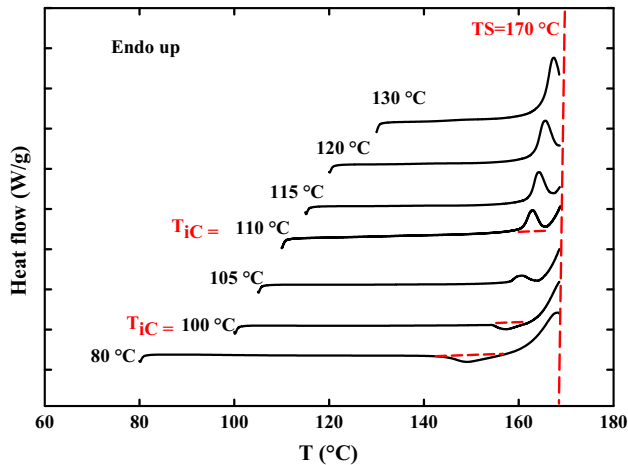
Figure 7 Heating scans obtained from various isothermal crystallization temperatures ranging from 80–140 °C to T_s = 170 °C at 2 °C/min. (Segment C in Fig. 2).
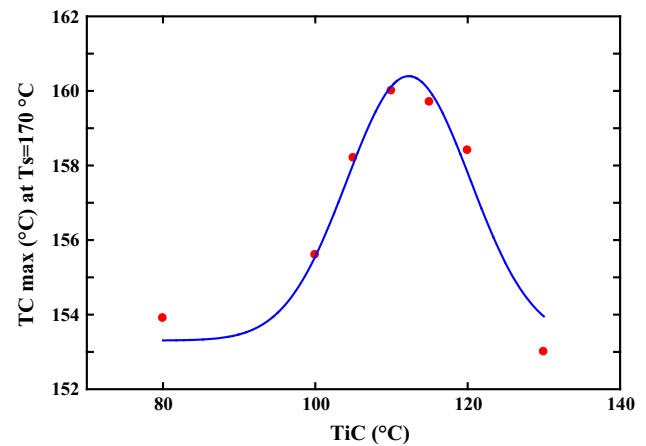

Figure 8 Maximum non-isothermal crystallization temperature, T_C^{max}, obtained after self-nucleation at T_s = 170 °C as a function of the crystallization temperatures, T_{iC}.

For all the investigated isothermal crystallization temperatures, Domain **II** was found to be located in the 170 °C ≤ T_s ≤ 174 °C temperatures range. Moreover, a significant effect of the initial crystallization temperature was obtained. Figure 8 exemplifies these effects by depicting T_C^{max} as a function of annealing temperature, T_{ic} for samples that were self-seeded at 170 °C. It was found that T_C^{max} displayed a clear maximum at T_{ic} = 110 °C. It is of immense surprise that T_{ic} revealed a large effect on the crystallization process since all crystals present at the end of self-seeding step are supposedly of α modification. One potential reason explaining this result might come from the nuclei density, N, and/or spherulite size, D, prior to self-nucleation. Isothermal crystallization experiments were, therefore, performed by optical microscopy and DSC to assess N and D.

Effect of T_{ic} on the nuclei density

To compare nuclei density of PLA crystallized at different isothermal crystallization temperatures (T_{ic}), the self-nucleated PLA specimens were quenched from T_s to 130 °C. Under isothermal conditions, nuclei density, N, can be derived by the well-known Avrami equation [37] which assumes that the relative crystallinity, $X(t)$, changes with the time t, according to the following equation:

$$1 - X(t) = \exp(-kt^n) \tag{1}$$

where n is the Avrami exponent and k is the crystallization rate constant. $X(t)$ can be calculated according to Eq. 2:

$$X(t) = \frac{\Delta H_t}{\Delta H_\infty} = \frac{\int_0^t \frac{dH}{dt} dt}{\int_0^\infty \frac{dH}{dt} dt}, \tag{2}$$

where ΔH_t and ΔH_∞ are the amounts of enthalpy generated at time t and infinite time, respectively, and $\frac{dH}{dt}$ is the enthalpy evolution rate. In order to graphically determine n and K, the Avrami equation is often written in the following form:

$$\ln[-\ln(1 - X(t)] = n \ln t + \ln k. \tag{3}$$

The crystalline fraction $X(t)$ is plotted in the form of $\ln[-\ln (1 - X(t)]$ versus $\ln t$ to yield the characteristic Avrami plot. The slope of this plot gives the Avrami constant n. The value of k is obtained by using the value of $X(t)$ at $t = t_{1/2}$, crystallization half-time. The crystallization half-time is defined as the time spent from the onset of the crystallization to the point where the crystallization is 50 % complete. The bulk crystallization rate can be deduced through the following equation:

$$k = \frac{\ln 2}{t_{1/2}^n}. \tag{4}$$

In the case of predetermined nucleation and three dimensional growth, the crystallization rate k is directly proportional to the total concentration of the number of nuclei, N, through Eq. 5:

$$N \approx \frac{3K}{4\pi G^3}, \tag{5}$$

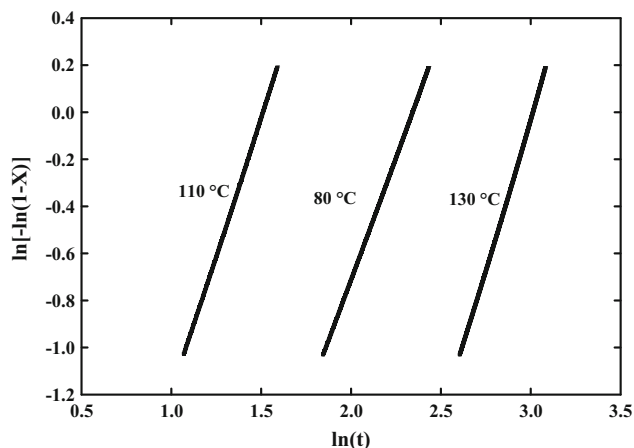where G is the spherulite growth rate measured by optical microscopy.

Figure 9 Plot of ln[−ln(1 − X)] versus ln t under crystallization at 130 °C for PLA that was first crystallized at the indicated T_{ic}, next self-nucleated at $T_s = 172$ °C, and finally cooled to 130 °C.

Table 2 Effect of isothermal crystallization temperatures, T_{ic}, on crystallization half-time, $t_{1/2}$, Avrami values, n and k, Nuclei density N, and average spherulite diameter D

T_{ic} (°C)	n	K (min^{-n})	$t_{1/2}$ (min)
80	2.15	0.00654	8.75
100	2.3	0.017	6.04
105	2	0.042	4.4
110	2.2	0.035	3.9
115	2.2	0.035	3.9
120	2.2	0.012	6.7
130	2.5	0.00045	17.7

As the value of N is obtained, the average spherulite size can also be determined according to the following equation [38]:

$$D = \left(\frac{6}{\pi N}\right)^{1/3}. \tag{6}$$

At first, an attempt was made to measure the Avrami parameters of the samples self-nucleated from $T_s = 170$ °C. The Avrami parameters for the sample self-nucleated at 170 and 171 °C could not be determined, because crystallization took place too fast and occurred during quenching. As a result, a value of $T_s = 172$ °C was selected. Figure 9 depicts the plot of ln[−ln (1 − X(t)] versus ln t for some samples self-nucleated at 172 °C. In all cases, the Avrami plots were linear confirming the applicability of the Avrami equation. Table 2 summarizes the effect of crystallization temperature T_{iC} on crystallization half-time, $t_{1/2}$ and Avrami parameters, (n and k). For all T_{ic}, the Avrami constant was very close to 2. The literature on PLA isothermal crystallization generally reports indexes between 2.5 and 4 [1]. Unfortunately, the morphology of the self-nucleated samples after cooling down to 130 °C could not be observed by optical microscopy due to small crystals size and high nucleation density. The different Avrami exponent may be due to the different nature of the crystal nuclei (i.e., Self-nucleation vs homogeneous and heterogeneous) and deserves further investigation. As T_{iC} increased from 80 to 105 °C, $t_{1/2}$ decreased from 8.8 to 4.4 min. These values then remained relatively constant up to 115 °C indicating that T_{iC} of 105–115 °C is optimal in terms of crystallization. The half-time increased again and K decreased for higher T_{iC} showing slower crystallization. It is important to mention here that these results do not represent the crystallization rate as a function of crystallization temperature as often found in the literature. Indeed, they present the effect of a prior crystallization prior to self-nucleation and further cooling. Nonetheless, the behavior is strikingly similar to that found when examining the effect of crystallization temperature on crystallization kinetics with an optimal crystallization temperature range in the 105–115 °C.

Figure 10 illustrates the variation of the average spherulite diameter, D, and nuclei density, N, versus the isothermal crystallization temperatures, T_{ic}, again for PLA being crystallized at 130 °C. The nuclei density exhibited a maximum at 110 °C that was about one order of magnitude higher than the value measured at 80 °C. The spherulite size was relatively constant at almost 50 microns between 105 and 115 °C and then increased rapidly to 220 microns at 130 °C.

Moreover, another intriguing phenomenon was found for samples that were initially crystallized at T_{ic} of 100–120 °C. When the samples were heated up to 173 °C for self-nucleation and then cooled down to check their crystallization (segment D in Fig. 2), two crystallization peaks upon cooling were found. This DSC cooling scan is shown in Fig. 11. Clear crystallization peaks at around 100 and 120 °C were found. So far, this peculiar behavior had not been reported for pure PLA containing heterogeneous nucleating agents. It might suggest that the crystallization mechanism is affected by the nature of nuclei (i.e., self-nucleated vs heterogeneous nuclei). Additionally, when the self-nucleation temperature was
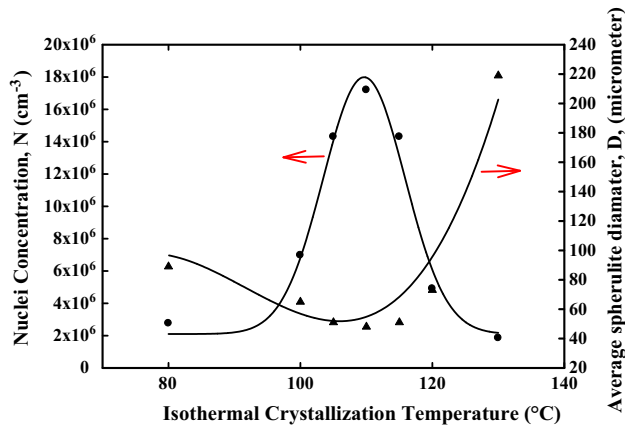
Figure 10 Variation of the nuclei density (*black circle*) and the average spherulite size (*black triangle*) of self-nucleated samples at $T_s = 172\ °C$ versus T_{ic}.
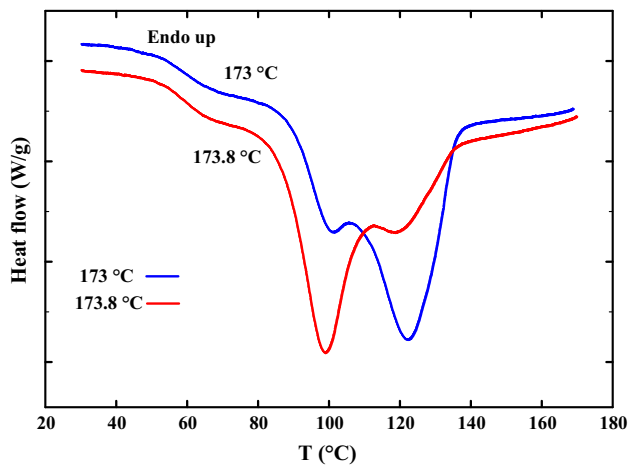

Figure 11 DSC cooling scans (Segment D in thermal protocol (Fig. 2) after self-nucleation at the indicated temperatures, T_s, for the samples were previously isothermally crystallized at 115 °C in the isothermal crystallization step.

Figure 12 XRD patterns of samples self-nucleated at indicated T_s, cooled at 2 °C/min, and then quenched: **a** after the first crystallization peak and **b** after the second crystallization peak. Note that the *arrows* indicate five characteristic peaks of the α phase.

minutely changed, the increases inside the self-seeding range from 173 to 173.8 °C: the 100 °C was favored over the 120 °C. These crystallization peaks could be associated to the formation of the α′ and α crystalline phases and shows how a minute change within self-nucleation temperature can result in significant changes in the mix of the α and α′ phases.

Microstructure analysis by WAXD

In order to characterize the structure during cooling when the double crystallization peaks were observed, XRD experiments were carried out. During cooling in
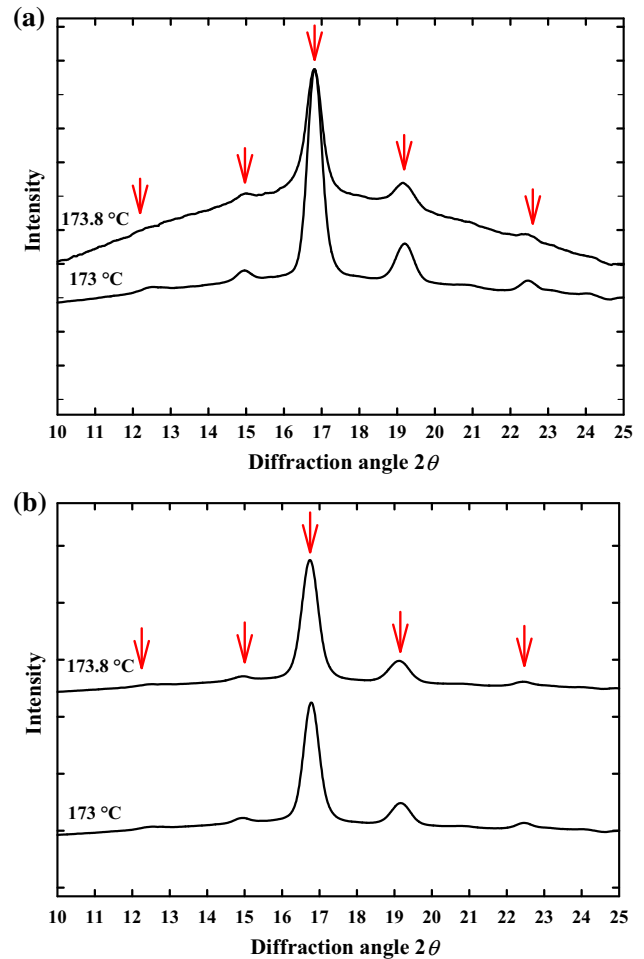
the DSC chamber, samples were taken out of the chamber and immediately quenched in cold water right after the first and second crystallization peaks. Figure 12 depicts the WAXD patterns of the samples after self-nucleation at 173 and 173.8 °C after the first (Fig. 12a) and second (Fig. 12b) crystallization peaks, respectively. As shown in Fig. 12a, after the first crystallization exotherm, both samples exhibited the characteristic diffraction peaks of the α phase. For the sample self-seeded at 173.8 °C, the level of crystallinity was smaller in agreement with the DSC results (c.f. Fig. 11). Figure 12b displays similar results but for the samples quenched after the second crystallization peak. The microstructures of all samples were rather similar, and differentiation between
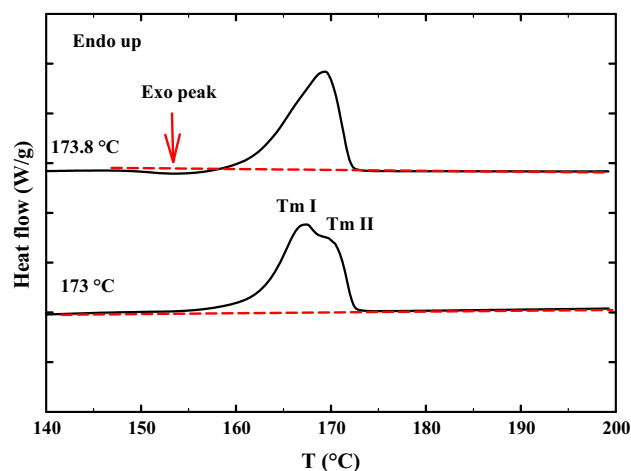
Figure 13 DSC heating scans at 2 °C/min in Segment E of the thermal protocol (Fig. 2) after cooling from the indicated self-nucleated temperatures, T_s.

the α and α′ phases was difficult. Therefore, thermal behavior of these mixed α and α′ samples upon heating was investigated.

DSC heating curves

In this section, we discuss about results obtained in segment E of the thermal protocol (Fig. 2) for the samples self-nucleated at 173 and 173.8 °C. It was observed in Fig. 13, upon heating at 2 °C/min, that the sample self-nucleated at 173.8 °C exhibited an exothermic peak prior to the single melting peak. As previously mentioned, this peak is associated to the α′-α solid-state transition. It indicates that in this sample, the fraction of the α′ phase was higher than that of α phase. Conversely, for the self-seeded sample at 173 °C, no exothermic peak was observed which implies that it possessed a higher α phase content. The later sample also exhibited the double melting peaks. The first melting peak, T_{mI}, is ascribed to melting of original α phase, whereas the second melting peak T_{mII} belongs to α′ crystals transformed to α phase through melt recrystallization. It was also observed that for the sample self-nucleated at 173 °C, the height of T_{mI} was higher than that of T_{mII}. It implies that more α phase was present. Structural evolution of the melt and cold crystallization of PLA has been investigated using FTIR, WAXD, and SAXS patterns by Wasanasuk et al. [39]. According to these authors, crystallization from the melt state does not lead directly to the α or α′ phases but instead to the formation of a mesomorphic phase prior to the

formation of α or α′ phases. Mesophase or meso-morphic phase is regarded as an intermediate state of matter between liquid and solid. In self-nucle-ation experiments, a self-nucleated polymer can be taken more or less as the mesophase. The conclusion that can be drawn from the double crystallization behavior is that the crystallization mechanism of self-nucleated PLA might differ from melt crystal-lized sample. It could also explain why PLA exhibited two peculiar crystallization peaks upon subsequent cooling, whereas this peculiarity has not been observed for samples directly cooled from the melt state.

Conclusions

A thermal procedure was designed to examine the self-nucleation behavior of PLA. Fully crystallized samples, previously isothermally crystallized between 80 and 130 °C, were self-nucleated near the melting temperature. Based on the non-isothermal crystallization temperature obtained upon cooling, three temperature domains were distinguished. In Domain **I**, the crystalline structure is completely destroyed. In Domain **II**, crystallization is nucleated by remaining crystals, and finally, in Domain **III**, crystallization proceeds by annealing of existing crystals. Domains **I, II**, and **III** were found for PLA as $T_s > 174$ °C, $170 \leq T_s \leq 174$, and $T_s < 174$ °C, respectively, where T_s is the self-nucleation temper-ature. Effect of crystalline modification on the self-nucleation of PLA was also investigated. It was observed that samples where a mixture of α and α′ crystal phases were generated exhibited the highest nucleation efficiency compared to samples isother-mally crystallized at temperatures leading to a single type of crystals. These samples also displayed the highest nuclei density and the smallest spherulite size. Furthermore, the samples, crystallized between 100 and 120 °C, exhibited two crystallization tem-peratures, around 100 and 120 °C, upon cooling after self-nucleation. In addition, by slightly changing the temperature within the self-nucleation temperature range, a change in the proportion of each peak was observed. It is for the first time that two exothermic peaks are reported for PLA upon cooling. These peaks were ascribed to α and α′ crystalline phases explaining the peculiar crystallization behavior of PLA.

Acknowledgements

References

[1] Saeidlou S, Huneault MA et al (2012) Poly(lactic acid) crystallization. Prog Polym Sci 37(12):1657–1677

[2] Mihai M, Huneault MA et al (2007) Extrusion foaming of semi-crystalline PLA and PLA/thermoplastic starch blends. Macromol Biosci 7(7):907–920

[3] Suryanegara L et al (2011) The synergetic effect of phenylphosphonic acid zinc and microfibrillated cellulose on the injection molding cycle time of PLA composites. Cellulose 18(3):689–698

[4] Zhai W et al (2009) A study of the crystallization, melting, and foaming behaviors of polylactic acid in compressed CO_2. Int J Mol Sci 10(12):5381–5397

[5] Kokturk G et al (2002) Evolution of phase behavior and orientation in uniaxially deformed polylactic acid films. Polym Eng Sci 42(8):1619–1628

[6] Li H, Huneault MA (2011) Comparison of sorbitol and glycerol as plasticizers for thermoplastic starch in TPS/PLA blends. J Appl Polym Sci 119(4):2439–2448

[7] Mihai M, Huneault MA, Favis BD (2009) Crystallinity development in cellular poly(lactic acid) in the presence of supercritical carbon dioxide. J Appl Polym Sci 113(5):2920–2932

[8] Li H, Huneault MA (2008) Crystallization of PLA/thermoplastic starch blends. Int Polym Proc 23(3):412–418

[9] Pantani R et al (2010) Crystallization kinetics of virgin and processed poly(lactic acid). Polym Degrad Stab 95(7):1148–1159

[10] Zhang J et al (2006) Confirmation of disorder α form of poly(L-lactic acid) by the X-ray fiber pattern and polarized IR/Raman spectra measured for uniaxially-oriented samples. Macromol Symp 242(1):274–278

[11] Zhang J et al (2005) Crystal modifications and thermal behavior of poly(l-lactic acid) revealed by infrared spectroscopy. Macromolecules 38(19):8012–8021

[12] Pan P et al (2008) Effect of crystallization temperature on crystal modifications and crystallization kinetics of poly(L-lactide). J Appl Polym Sci 107(1):54–62

[13] Pan P et al (2008) Polymorphic transition in disordered poly(l-lactide) crystals induced by annealing at elevated temperatures. Macromolecules 41(12):4296–4304

[14] Pan P et al (2007) Polymorphous crystallization and multiple melting behavior of poly(l-lactide): molecular weight dependence. Macromolecules 40(19):6898–6905

[15] Zhang J et al (2008) Disorder-to-order phase transition and multiple melting behavior of poly(l-lactide) investigated by simultaneous measurements of WAXD and DSC. Macromolecules 41(4):1352–1357

[16] Kawai T et al (2007) Crystallization and melting behavior of poly (l-lactic acid). Macromolecules 40(26):9463–9469

[17] Kalish JP et al (2011) Spectroscopic and thermal analyses of α' and α crystalline forms of poly(l-lactic acid). Polymer 52(3):814–821

[18] Chen X, Kalish J, Hsu SL (2011) Structure evolution of α'-phase poly(lactic acid). J Polym Sci Part B Polym Phys 49(20):1446–1454

[19] Li H, Huneault MA (2007) Effect of nucleation and plasticization on the crystallization of poly(lactic acid). Polymer 48(23):6855–6866

[20] Fillon B et al (1994) Efficiency scale for polymer nucleating agents. J Therm Anal Calorim 42(4):721–731

[21] Fillon B et al (1993) Self-nucleation and enhanced nucleation of polymers. Definition of a convenient calorimetric "efficiency scale" and evaluation of nucleating additives in isotactic polypropylene (α phase). J Polym Sci Part B Polym Phys 31(10):1395–1405

[22] Fillon B et al (1993) Self-nucleation and recrystallization of isotactic polypropylene (α phase) investigated by differential scanning calorimetry. J Polym Sci Part B Polym Phys 31(10):1383–1393

[23] Lotz B (1998) α and β phases of isotactic polypropylene: a case of growth kinetics phase reentrency in polymer crystallization. Polymer 39(19):4561–4567

[24] Fillon B et al (1993) Self-nucleation and recrystallization of polymers. Isotactic polypropylene, β phase: $\beta - \alpha$ conversion and $\beta - \alpha$ growth transitions. J Polym Sci Part B Polym Phys 31(10):1407–1424

[25] Schneider S et al (2001) Self-nucleation and enhanced nucleation of polyvinylidene fluoride (α-phase). Polymer 42(21):8787–8798

[26] Marquez L, Rivero I, Müller AJ (1999) Application of the SSA calorimetric technique to characterize LLDPE grafted with diethyl maleate. Macromol Chem Phys 200(2):330–337

[27] Arnal M et al (2000) Applications of successive self-nucleation and annealing (SSA) to polymer characterization. J Therm Anal Calorim 59(1):451–470

[28] Michell RM et al (2010) Effect of sequence distribution on the isothermal crystallization kinetics and successive self-nucleation and annealing (SSA) behavior of poly(ε-caprolactone-co-ε-caprolactam) copolymers. Eur Polym J 46(6):1334–1344

[29] Schmidt SC, Hillmyer MA (2001) Polylactide stereocomplex crystallites as nucleating agents for isotactic polylactide. J Polym Sci Part B Polym Phys 39(3):300–313

[30] Anderson KS, Hillmyer MA (2006) Melt preparation and nucleation efficiency of polylactide stereocomplex crystallites. Polymer 47(6):2030–2035

[31] De Santis F, Pantani R, Titomanlio G (2011) Nucleation and crystallization kinetics of poly(lactic acid). Thermochim Acta 522(1–2):128–134

[32] Androsch R, Iqbal HMN, Schick C (2015) Non-isothermal crystal nucleation of poly (l-lactic acid). Polymer 81:151–158

[33] Saeidlou S et al (2012) Evidence of a dual network/spherulitic crystalline morphology in PLA stereocomplexes. Polymer 53(25):5816–5824

[34] Sabino MA, Ronca G, Müller AJ (2000) Heterogeneous nucleation and self-nucleation of poly(p-dioxanone). J Mater Sci 35(20):5071–5084

[35] Sabino MA, Feijoo JL, Müller AJ (2000) Crystallisation and morphology of poly(p-dioxanone). Macromol Chem Phys 201(18):2687–2698

[36] Yasuniwa M et al (2008) Melting behavior of poly(l-lactic acid): X-ray and DSC analyses of the melting process. Polymer 49(7):1943–1951

[37] Avrami Melvin (1939) Kinetics of phase change-I. Gen Theory J Chem Phys 7:1103–1109

[38] Supaphol P, Spruiell JE (2000) Crystalline memory effects in isothermal crystallization of syndiotactic polypropylene. J Appl Polym Sci 75(3):337–346

[39] Wasanasuk K, Tashiro K (2011) Structural regularization in the crystallization process from the glass or melt of poly(l-lactic acid) viewed from the temperature-dependent and time-resolved measurements of FTIR and wide-angle/small-angle X-ray scatterings. Macromolecules 44(24):9650–9660